Analysis of Caveolin-1 Expression and Interaction with FSHR in Lipid Raft Domains

By

Joseph Bott

****

Submitted in partial fulfillment
of requirements for
Honors in the Department of
Biology

UNION COLLEGE

JUNE, 2021

Abstract

Bott, Joseph Analysis of Caveolin-1 Expression and Interaction with FSHR in Lipid Raft Domains. Department of Biology, June 2021
ADVISOR: Brian D. Cohen

For thousands of women in the United States ovarian cysts, tumors, and hormonal imbalances contribute to reduced fertility and fecundity. In addition to these factors, many other unexplained physiological mechanisms may play a role in women's reproductive health. Specifically, human follicle stimulating hormone (hFSH) binds to a G protein coupled receptor (GPCR) called human follicle stimulating hormone receptor (hFSHR). This interaction helps to regulate the reproductive system in both males and females indicating that it may be a key player to target in order to promote fertility. Previous work in our lab has demonstrated that hFSHR, like other GPCR, has been shown to preferentially localize within microdomains in the cell membrane known as lipid rafts in order to facilitate proper signaling. This localization is thought to be mediated in part by a protein known as caveolin. In order to investigate the relationship hFSHR and caveolin, a cell line expressing hFSHR (HEK293-hFSHR) was transfected with a plasmid to transiently express caveolin. Immunoprecipitations were used to investigate the interaction between caveolin and full length hFSHR. Western blot analysis was subsequently performed to detect protein interactions. Based on the data generated from this experiment, the previously established relationship between FSHR and lipid raft residency was not confirmed because it was not shown that caveolin co-precipitated with FSHR. These findings may suggest that previous studies used methods that resulted in artifactual phenomenon. However, it is equally possible that the conditions, plasmids, or cells used in these experiments contributed to the inability to replicate the results found previously. Understanding the possible interaction between hFSHR and caveolin is crucial in the future development of therapeutics that will allow us to fine tune receptor function for infertility treatments.

Acknowledgments

I would like to acknowledge my thesis advisor and mentor Professor Brian Cohen. He has provided instrumental guidance, scholarly advice, and encouragement throughout my research and career at Union College. I would also like to thank all of the members of Team Cohen for their collective contributions to my studies. To the Union College Biology and Chemistry Departments, thank you all for instilling in me the spirit of discovery and passion for the sciences. Finally, I would like to thank my mother Lia, and my sister Aria, for giving their opinions and love throughout my academic endeavors.

Introduction

According to the Society of Reproductive Surgeons, 6.7 million women in the US face difficulties conceiving. In 2019, roughly six percent of married American women aged 15 to 44 suffered from infertility, while about 12 percent of all American women in the same age group suffered from impaired fecundity (1). Impaired fecundity refers to the inability to become pregnant whereas infertility refers to difficulty becoming or staying pregnant. The male partner is solely responsible for failure to conceive for about eight percent of couples (1). Current techniques designed to help couples conceive and carry to term include, but are not limited to pharmacological intervention, surgery, artificial reproductive technology (ART), and artificial insemination. Surgical techniques such as ovarian cyst or tumor removal aim to remove potential

physical barriers that otherwise prevent normal menses and sometimes restore distorted hormone levels. Medications prescribed usually supplement reproductive hormones whose production is nonexistent. For example, the medication Letrozole works by promoting ovulation by reducing estrogen production thus correcting issues within the female hormone signaling pathways (2).

However, such interventions are not always effective because there are multiple, not fully understood, influences. Many unexplored factors potentially contribute to infertility and/or decrease fecundity for many couples. Developing pharmaceutical interventions to combat infertility is paramount. A 2010 study suggested that pharmacological intervention offers a far less expensive solution to promote conception. It found that the annual cost of medication for women undergoing infertility treatments was $1,182, while the average total cost for a woman to successfully conceive in 18 months or less using IVF was over $61,000 (3). The key to unlocking new tools to reduce infertility and promote fecundity is by further studying reproductive hormones and their functions. One such reproductive hormone is follitropin (FSH).

FSH is a regulatory hormone in the hypothalamic-pituitary-gonadal (HPG) axis, which as one of its roles, helps to regulate the reproductive system in both males and females. The hypothalamus, as part of the HPG axis, is the neural control center in the forebrain that regulates temperature control, hunger, thirst, and circadian rhythms through hormonal secretions. The pituitary gland, located below the hypothalamus in the midbrain, is composed of many tissues and is responsible for the production of FSH. When stimulated by gonadotropin-releasing hormone secreted from the hypothalamus, gonadotropic tissue in the anterior pituitary releases

gonadotropin hormones that include human luteinizing hormone (hLH), and human follicle stimulating hormone (hFSH).

In women, hFSH and hLH both act on the follicular cells of the ovaries to promote follicle maturation. Follicles are small sacs within the ovaries that are necessary to support developing egg cells (4) (Figure 1). Progesterone, whose production is also stimulated by hFSH and hLH activity, signals for growth of the endometrium in the uterus to prepare for egg implantation. As follicles mature, they produce inhibin, which acts to decrease hFSH production in the anterior pituitary. An hLH surge during the menstrual cycle causes a follicle to burst resulting in the release of an egg during ovulation. Post-ovulation, the corpus luteum produces progesterone inhibiting hFSH, hLH, and GnRH production (5) (Figure 2). Studies have shown that women lacking this FSH action are infertile (6).

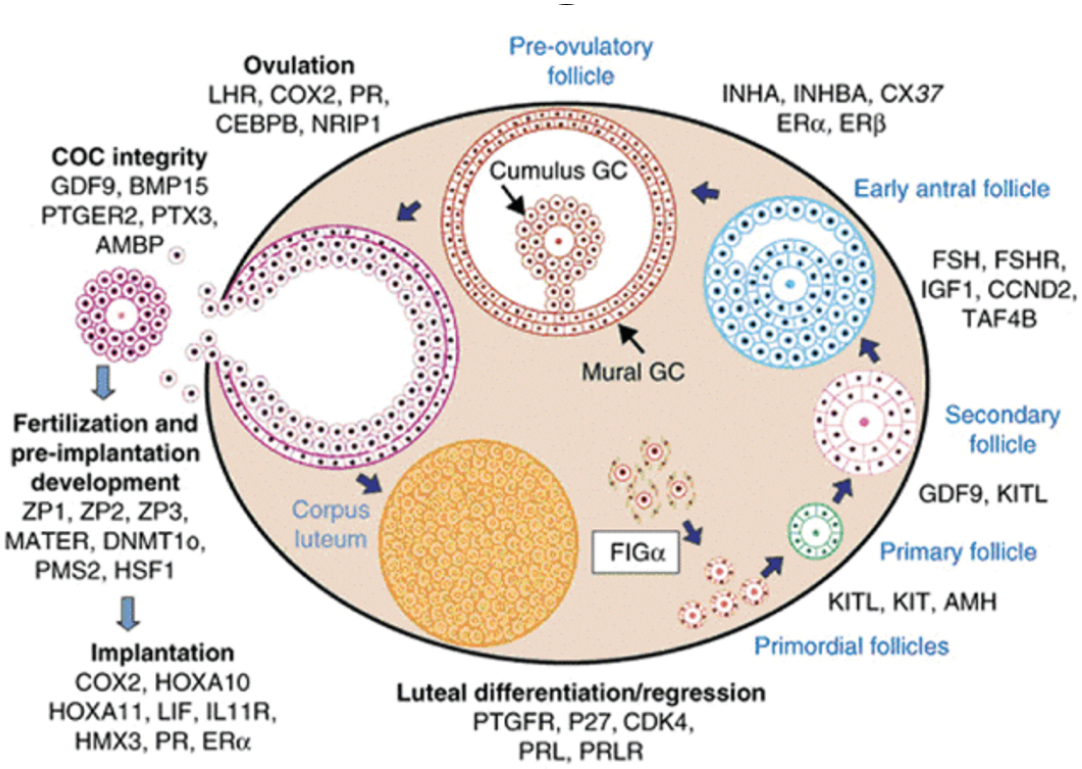

MM Matzuk, DJ Lamb: Nat cell Biol 4:Suppl S41-9, 2002

Figure 1. Follicular maturation and formation of the corpus luteum.

In males, FSH regulates Sertoli cell proliferation and differentiation in the immature testis and influences various functions of these cells in adult life, thus indirectly maintaining spermatogenesis. Unlike in women, a lack of FSH action in males appears to only partially impair fertility (6).

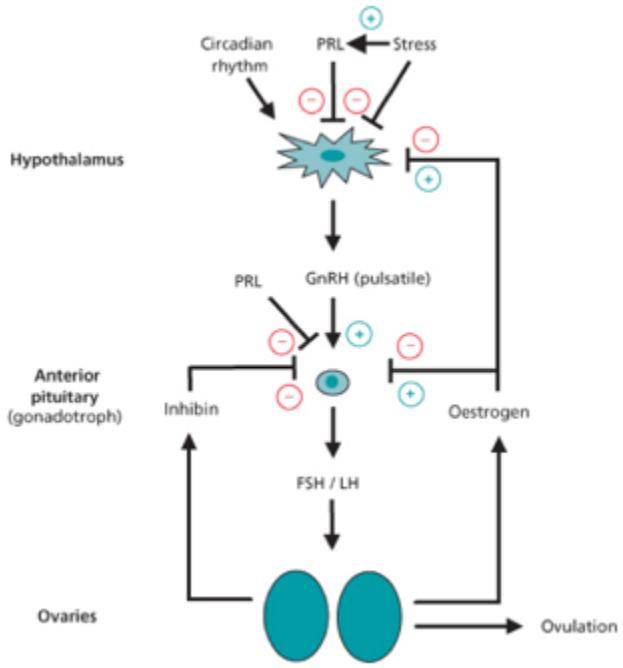

G., H. R. I., & Hanley, N. A. (2012). *Essential endocrinology and diabetes: Richard Ig Holt ; Neil A Hanley* (6th ed.). Wiley-Blackwell.

Figure 2. Hormonal regulation of the female reproductive system. Red minus signs indicate inhibition. Blue plus signs indicate activation.

Specific interactions between hormones and their receptors can elicit a large spectrum of biochemical responses within the target cells. Without its corresponding receptor, hormones are unable to perform their physiological function. hFSH binds specifically to an extracellular

domain of G protein-coupled receptors known as human follicle stimulating hormone receptor (hFSHR) (6) (Figure 3A). hFSHR contains 7-transmembrane domains, an extracellular domain that receives signals from the cell's environment, and an intracellular domain that facilitates the propagation of the extracellular signal to the interior of the cell (6) (Figure 3B). Like most G protein-coupled receptors, the intracellular domain interacts with a heterotrimeric G protein. When the extracellular domain of hFSHR binds to hFSH, the intracellular domain catalyzes the exchange of a guanosine diphosphate (GDP) molecule for a guanosine triphosphate (GTP) molecule bound to the alpha subunit of the heterotrimeric G protein. Eventually, a subunit of the G protein will catalyze the hydrolysis of GTP to GDP and Pi. The Pi unit then activates a signaling cascade intracellularly. The G protein remains in a heterotrimeric state, bound to GDP, until the G protein-coupled receptor is activated to catalyze the exchange of GDP for GTP again (7).

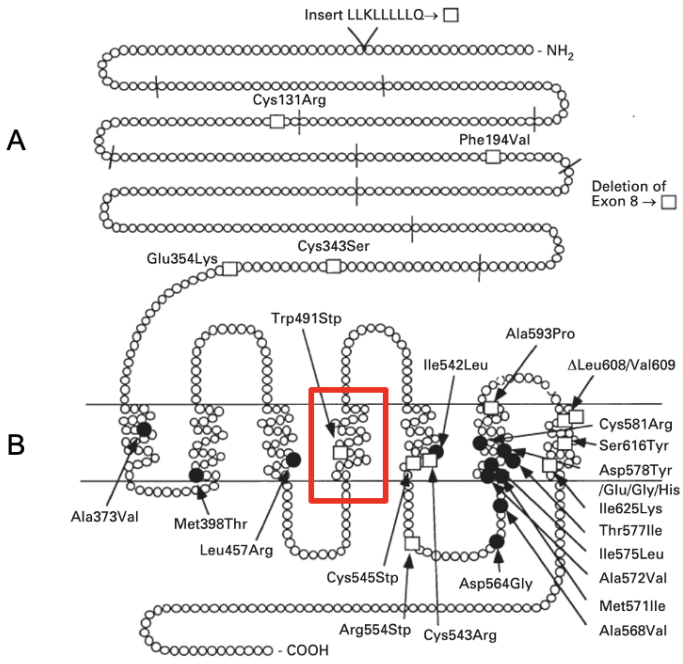

Huhtaniemi I. The Parkes lecture. Mutations of gonadotrophin and gonadotrophin receptor genes: what do they teach us about reproductive physiology? J Reprod Fertil. 2000

Figure 3. Human FSHR with combined caveolin binding motif circled in red.

The specific intracellular signaling pathways activated through hFSH-hFSHR interaction are complex and not fully understood. It is generally accepted that adenosine triphosphate (ATP) is activated by adenylyl cyclase. Once activated, ATP is converted to cyclic adenosine monophosphate (cAMP) which then allows for the phosphorylation of the cAMP response element binding protein (CREB) to phospho-CREB by protein kinase A (8). hFSHR signaling also leads to beta-arrestin activation which leads to the activation of the MAPK pathway. This results in the phosphorylation of p44 to phospho-p44 (8). Because cAMP, phospho-CREB, and phospho-p44 can be detected in biochemical assays, they are commonly used as intracellular markers to detect hFSHR signaling.

Previous work in our lab has demonstrated that human FSHR (hFSHR), like other GPCRs, has been shown to preferentially localize within microdomains in the cell membrane known as lipid rafts in order to facilitate proper signaling (9) (10) (Figure 4). Lipid rafts are areas of the cell membrane that demonstrate high rigidity and resistance to detergents. These properties are due to the presence of higher concentrations of sphingolipids and cholesterol than in the surrounding membrane (9). The uniquely dense membrane composition of lipid rafts is thought to facilitate colocalization of signaling components which modulates the signaling ability of cells (11). For example, researchers found that IgE signaling in basophil cells is more efficient when coordinated via lipid rafts (11). In places where the protein caveolin is present, the lipid raft can exist as flask shaped invaginations known as caveolae (12). It has been suggested that caveolin, a scaffolding protein, plays a critical role in hFSHR transit into and out of lipid rafts. A study

using caveolin knockout mice further supports the idea that caveolin plays a role in regulating signal transduction. In the study, knockout mice deficient in caveolin-1, -2, and -3 were generated. Pathologies related to signaling molecules and ion channels were induced in their cardiovascular, pulmonary, urogenital, skeletal, neural, and endocrine systems, as well as increased susceptibility to cancer (13).

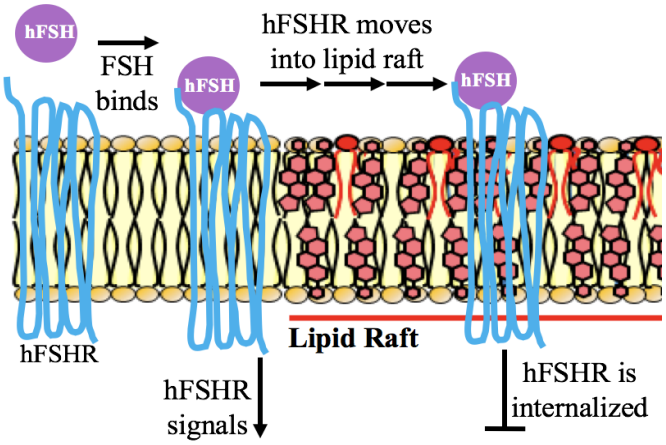

Wells, M., & Cohen, B. D. (2018). Follicle Stimulating Hormone Receptor Signaling is Regulated by Lipid Raft Residency. *The FASEB Journal*.

Figure 4. hFSHR motility in lipid rafts to facilitate signaling.

Although the specific function of the caveolin-hFSHR interaction is not well understood, our preliminary data also suggests that caveolin is physically associated with hFSHR. We hypothesize that for hFSHR to localize within lipid rafts and caveolae, it must interact with caveolin through a specific sequence in the protein known as the caveolin binding motif (CBM) (circled in Figure 3 and shown below in Figure 5). This protein sequence is frequently found in proteins that interact with caveolin, which may suggest that the hFSHR sequence plays an important role in the hFSH signaling pathway (14) (Table I). The CBM is known to have four aromatic residues (φ in the sequence in Figure 5). This sequence of ten amino acids in the CBM

follows a φXφXXXXφXXφ pattern, which are considered to be the functional units of this motif. In the case of FSHR, all φ's correspond to a phenylalanine (14).

Table I. List of proteins containing CBM sequence that are thought to interact with caveolin-1.

Caveolin associated molecule	CBM sequences and location (aromatic positions emboldened)	Experimental mutation of CBM	Confirmation of structural integrity of mutant	References
Protein kinase Cγ	539-**W**S**F**GVLL**Y**-546	No	–	[97]
	673-**FTY**VNPD**F**-680	No	–	
Protein kinase Cζ	428-**Y**G**F**SVDW**W**-435	No	–	[96]
Ptc	788-**Y**D**F**IAAQ**F**K**Y**F-798	Yes	No	[98]
PTEN	271-**F**H**F**WVNT**F**-278	Yes	No	[39]
PTPN1	174-**F**HYTT**W**PD**F**-182	No	–	[99]
PTPN6	206-**F**V**Y**LRQP**Y**-213	No	–	[99]
PTPN11	420-**W**Q**Y**HFRT**W**-427	No	–	[99]
Recoverin	65-**Y**AQHY**F**RS**F**-73	No	–	[100]
Rho-associated protein kinase 1	135-**W**VVQL**F**CA**F**-143 148-**Y**L**Y**MVME**Y**-155	No	–	[101]
Rho-related GTP binding protein RhoC	34-**Y**VPTV**F**EN**Y**-42	No	–	[102]
Sialidase-3	179-**YTY**YIPS**W**-186	Yes	No	[36]
SKR3	399-**W**A**F**GLVL**W**-406	Yes	No	[32]
Slo1	1130-**Y**NMLC**F**GI**Y**-1138	Yes	Yes (Sucrose gradient)	[30,44]
Sodium/calcium exchanger 1	259-**Y**KYV**Y**KR**Y**-266	No	–	[103]
	654-**YLF**GQPV**F**-661	No	–	
Sodium/potassium-transporting ATPase subunit alpha-1	92-**F**CRQL**F**GG**F**-100 987-**W**W**F**CAFP**Y**-994	Yes	No	[104,105]
Solute carrier family 22 member 11	158-**F**I**W**GLLS**Y**-165	No	–	[106]
Solute carrier family 22 member 8	216-**YCY**TFGQ**F**-223	No	–	[107]
Striatin	55-**F**LQHE**W**AR**F**-63	No	–	[108]
Striatin-4	71-**F**IQHE**W**AR**F**-79	No	–	[108]
Sulphonylurea receptor 2B	138-**FLY**WVMA**F**-145	No	–	[109]
TLR4	1146-**FY**F**I**QKY**F**-1153	No	–	[110]
TNF receptor associated factor 2	354-**F**I**W**KISD**F**-361	No	–	[111]
Transforming protein RhoA	34-**Y**VPTV**F**EN**Y**-42	No	–	[22]
TrpC1	781-**F**RTSK**Y**AM**F**-789	Yes	No	[84,112]
Type-1 angiotensin II receptor	302-**YGF**LGKK**F**KR**Y**-312	Yes	No	[61,113]
VEGFR-2	1089-**WSF**GVKK**W**EI**F**-1099	No	–	[114]
VEGFR-3	1098-**WSF**GVLL**W**EI**F**-1108	No	–	[115]

Dominic PB, Dart C, Daniel JR. Evaluating Caveolin Interactions: Do Proteins Interact with the Caveolin Scaffolding Domain through a Widespread Aromatic Residue-Rich Motif? PLoS One. 2012 Sep 1,;7(9):e44879.

Similarly, hFSHR has four key phenylalanine residues in the fourth transmembrane domain (F- circled in Figure 3) that are consistent with the CBM. The aromatic residues in this motif are colloquially referred to as the A, B, C, and D sites. The residues are located at positions 479, 481, 486, and 489, respectively. When viewed in a three-dimensional model, the B site is oriented opposite from the A, C, and D sites. This suggests that the B site may play a minor role in the function of this motif due to its isolation from the other aromatic amino acids (Figure 5).

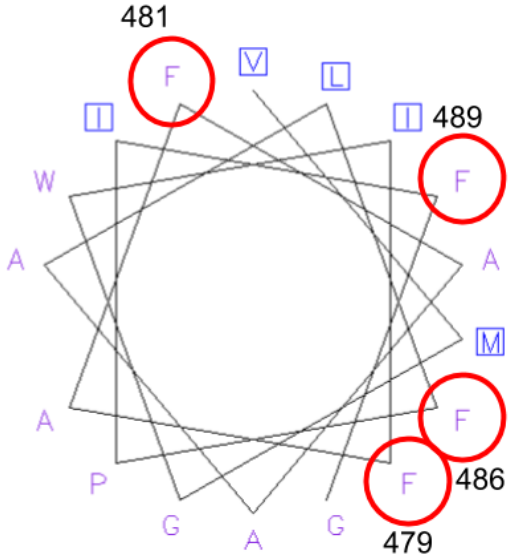

Caveolin Binding Motif: Wild Type (WT):	φXφXXXXφXXφ FAFAAALFPIF

Created by Professor Brian D. Cohen.

Figure 4. Helical wheel diagram depicting the CBM of hFSHR with the location of the four aromatic residues labeled.

Based on prior data suggesting that hFSHR signaling is regulated by lipid raft residency and the results suggesting a possible role of caveolin in the regulation, this study aimed to further validate the role of lipid rafts and caveolin in hFSHR signaling regulation. We specifically investigated caveolin interaction with full length receptors by performing immunoprecipitations.

In our experiments, we first performed western blot analysis of whole cell extract experiments. Then, we attempted to co-immunoprecipitate hFSHR and caveolin-1 out of solution using specific antibodies. Previous experiments done in our lab, provide substantial evidence to

suggest that western blot analysis will definitively show that the hFSHR and caveolin-1 are in physical interaction with each other.

Methods

HEK293-hFSHR cells expressing hFSHR were grown to confluence in Corning cell culture flasks using a Dulbecco's Modified Eagle Medium (DMEM) and the antibiotic G418. Transfections were performed on cells in 60 mm dishes as described in the transit 293 protocol (Appendix I).

Whole cell extracts were harvested by washing each dish in 1 mL ice cold PBS. Then, 1 mL ice cold PBS/EDTA was added to each dish and allowed to incubate for 5 minutes. The cells were collected in microfuge tubes and centrifuged at max speed at 4° C for 20 minutes. Pellets were resuspended in either 1 mL of CHAPS or Octylglucoside buffer. Recipes for the buffers can be found in Appendices II and III respectively. The microfuge tubes were vortexed and centrifuged at max speed at 4° C for 20 minutes. The supernatant was transferred to a new tube.

Cells were harvested for co-immunoprecipitations by first placing the 60 mm dishes on ice. The dishes were washed with 1 mL of ice cold PBS. Then, 1 mL of ice cold lysis buffer was added to the dishes and allowed to incubate for 20 minutes. The cells were scraped and collected in microfuge tubes. The samples were transferred from the microfuge tubes to dounce homogenizers. The samples were transferred back to the microcentrifuge tubes and were then centrifuged at max speed at 4° C for 30 minutes. The supernatant was transferred to a new tube.

Alternatively, octylglucoside and CHAPS were sometimes used in place of lysis buffer during cell harvesting.

The gel electrophoresis was conducted at 100V for approximately two hours using 1X running buffer. The “Good Mojo” Protocol was followed to develop the western blots after performing SDS-PAGE gel electrophoresis (Appendix V). Alternatively, another protocol for developing membranes was used when probing with caveolin-1 specific antibody (Appendix VI).

Results and Discussion

Western blot analysis of whole cell extract was performed on two membranes probed with biotinylated anti-FSHR antibody and biotinylated anti-myc antibody that bound to myc-tagged caveolin expressed by cultured cells (Figure 5). The left membrane was probed with biotinylated anti-FSHR antibody and the right membrane was probed with biotinylated anti-myc antibody. The left blot shows the presence of FSHR indicated by the blue box. These bands are consistent with what we would have expected because both lanes two and four were loaded with samples that supposedly contained FSHR. In the right blot, bands consistent with caveolin-1 were present. Consistent with our prediction, bands were present in the lane that contained the sample transfected with caveolin-1 and not in the lane loaded with samples transfected with empty vector. This experiment supports the conclusion that both FSHR and caveolin-1 are expressed in the cells cultured in the lab. In order to confirm this finding, this experiment was repeated using non-biotinylated antibodies.

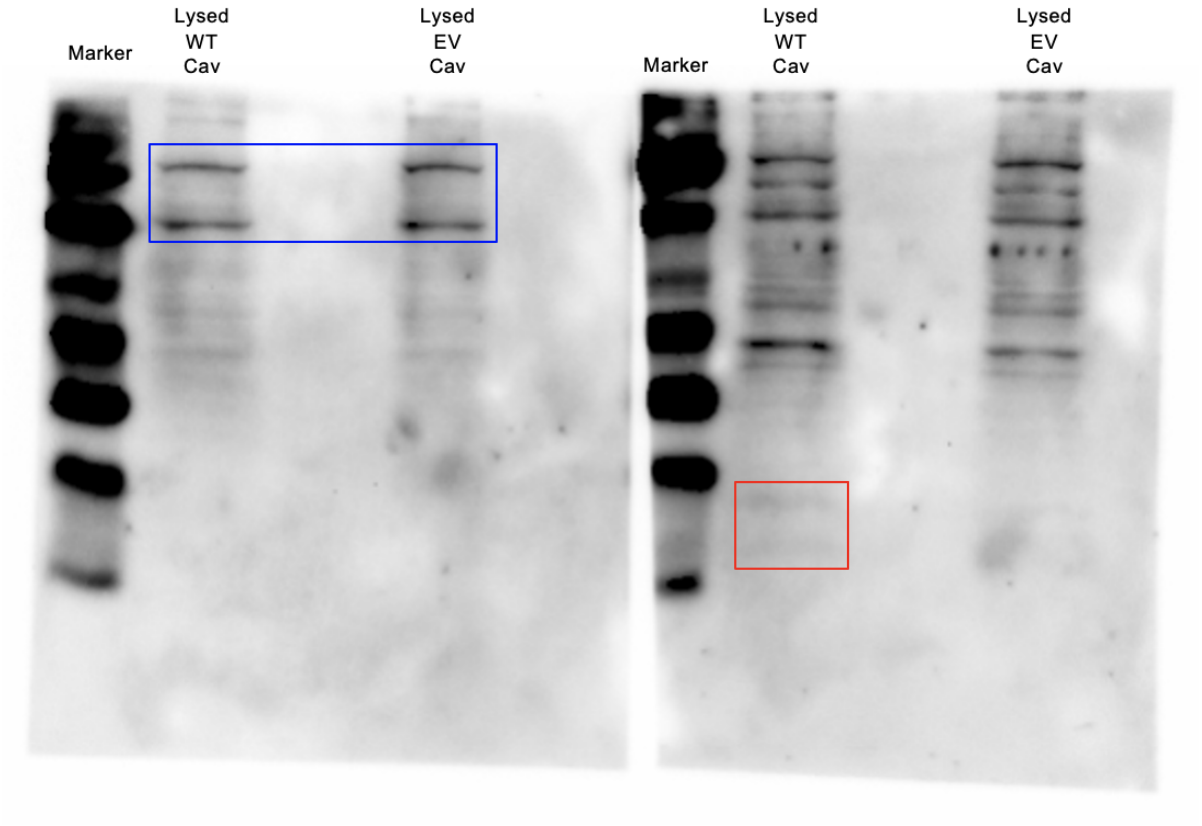

Figure 5. Western blot analysis of whole cell extracts experiments. (Left Membrane) Membrane was probed with biotinylated anti-FSHR antibody. Lanes are 1. Molecular weight marker, 2. Cav+/Lysis buffer, 4. Cav-/Lysis buffer. (Right Membrane) Membrane was probed with biotinylated anti-caveolin antibody. Lanes are Lanes are 1. Molecular weight marker, 2. Cav+/Lysis buffer, 4. Cav-/Lysis buffer. Blue box indicates presence of receptor. Red box depicts caveolin protein.

A western blot analysis of whole cell extracts was performed using non-biotinylated antibodies to demonstrate the expression of both FSHR and caveolin-1 in cells cultured in the lab (Figure 6). The top blot was probed with a caveolin-1 specific antibody. The red box represents the region where bands consistent with caveolin-1 might be present. In lanes two-five, caveolin-1 appeared to be present which is consistent with the expected results. Similar bands did not appear to be present in lanes six-nine. This indicates that caveolin-1 was not present. This finding is consistent with the expected results because these lanes contained samples that were transfected with an empty vector. The bottom blot was probed with an anti-FSHR antibody. Bands consistent with FSHR were present in all lanes. It is interesting to note that the density of the bands were

not uniform. Although an explanation for this phenomena is not available at this time, it is possible that the lanes were not loaded with a consistent amount of sample. Thus, some bands appear darker or lighter than others because of the amount of protein present. Overall, this experiment confirmed the presence of FSHR and caveolin-1 in the cells cultured in the lab.

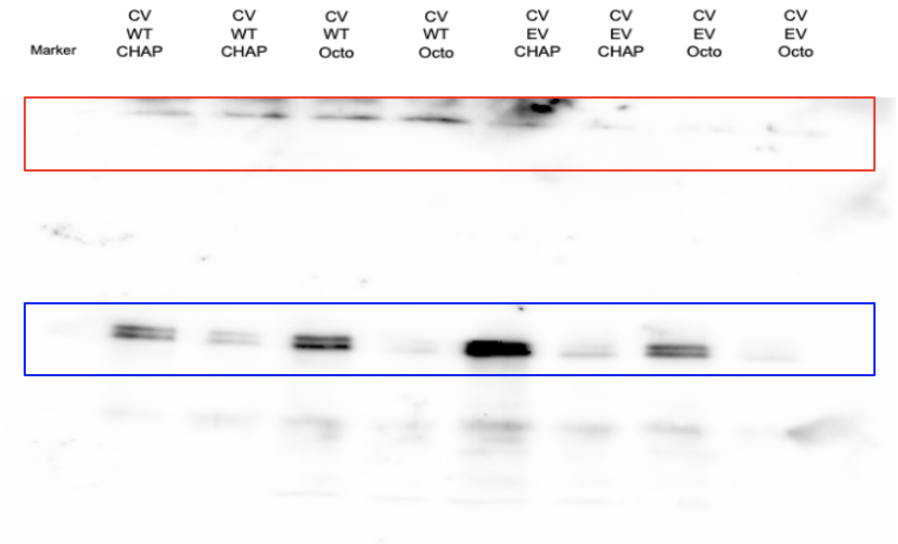

Figure 6. Western blot analysis of whole cell extracts experiments. Lanes are 1. Molecular weight marker, 2. Cav+/IgG/CHAPS buffer, 3. Cav+/CHAPS/mAb105, 4. Cav+/IgG/Octylglucoside buffer. 5. Cav+/mAb105/Octylglucoside buffer, 6. Cav-/IgG/CHAPS buffer, 7. Cav-/mAb105/CHAPS buffer, 8. Cav-/IgG/Octylglucoside buffer, 9. Cav-/mAb105/Octylglucoside buffer. The top membrane was incubated with an anti-caveolin antibody. The bottom membrane was incubated with an anti-FSHR antibody.

In order to demonstrate the existence of a physical association between FSHR and caveolin-1, a western blot analysis of co-immunoprecipitation experiments was performed using non-biotinylated antibodies (Figure 7.) Samples incubated with IgG should not produce bands that are consistent with receptor being present. Samples incubated with 105, the antibody that binds to FSHR, should produce bands that are consistent with receptor being present. All samples transfected with wild type caveolin and probed with a FSHR specific antibody may or may not produce bands that are consistent with a caveolin and FSHR co-immunoprecipitation. All other lanes should not show bands consistent with caveolin-1.

The top blot was probed with anti-caveolin-1 antibodies. Bands, boxed in blue, occurred in lanes four, five, and seven indicating the presence of light-chain antibodies. In addition, darker bands, boxed in red, presented in lanes four, five, and seven. These bands are consistent with the presence of heavy-chain antibody. Caveolin-1 should have been present around 20 kD in lanes three, five, seven, and eight. However, caveolin-1 was not detected in any of the lanes.

The bottom blot was probed with an anti-FSHR antibody. Bands boxed in red presented in lanes four, five, and seven. They are indicative of light-chain antibodies. Darker bands boxed in blue presented in lanes four, five, and seven also. They are indicative of heavy-chain antibodies. Interestingly, FSHR bands were not present in any lanes on this blot. They should have been present at a higher molecular weight than the heavy-chain antibodies. Without detecting the presence of receptor or caveolin-1 in any of the two blots, no conclusion can be drawn as to whether caveolin-1 physically interacts with FSHR because the two moieties did not co-immunoprecipitated together.

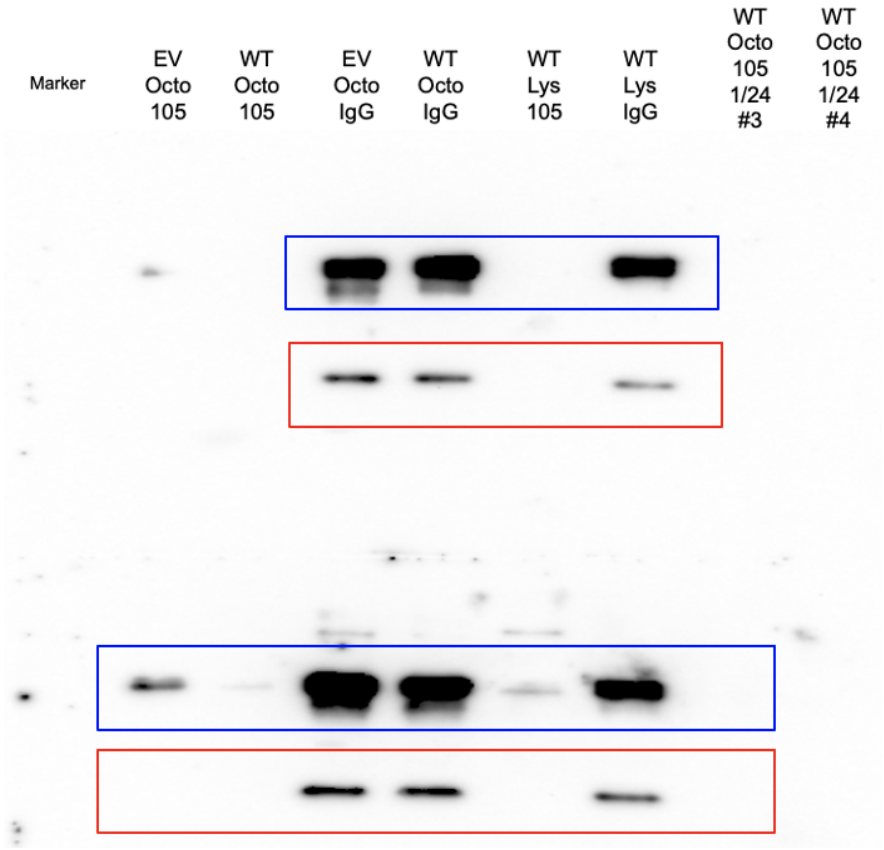

Figure 7. Western blot analysis of co-immunoprecipitation experiments where lanes are; 1. Molecular weight marker, 2. CAV-/mAb105/Octylglucoside buffer, 3. Cav+/mAb105/Octylglucoside buffer, 4. CAV-/IgG/Octylglucoside buffer, 5. Cav+/mAb105/Octylglucoside buffer, 6. CAV-/mAb105/Lysis buffer, 7. CAV-/IgG/Octylglucoside buffer, 8. Cav+/mAb105/Octylglucoside buffer (Sample 1), 9. Cav+/mAb105/Octylglucoside buffer (Sample 2). The top membrane was incubated with an anti-caveolin antibody. The bottom membrane was incubated with an anti-FSH antibody.

In order to confirm the previous findings, the co-immunoprecipitation experiment was repeated. Again, a western blot analysis of the samples obtained from the co-immunoprecipitation experiments was performed using non-biotinylated antibodies (Figure 8) The top blot was probed with a caveolin-1 specific antibody. Bands present in lanes four and five were boxed in red. Most likely, these bands are indicative of non-dissociated heavy and light-chain antibodies because they occurred in the IgG lane. These bands probably presented because the sample was not heated for long enough after performing the co-immunoprecipitation. Dark bands that presented in lanes four, five, eight, and nine were

boxed in blue. These bands are consistent with the presence of heavy-chain antibodies. As in the previous experiment, bands consistent with caveolin-1 did not present. The bottom blot was probed with an anti-FSHR specific antibody. By in-large the bottom blot contained the same bands as the blot probed with caveolin-1 did. Both bands consistent with non-dissociated heavy and light-chain antibodies, as well as heavy-chain antibodies were present. Bands consistent with FSHR were not detected. As a result, the previous data were confirmed and no conclusion could be made about the physical association between FSHR and caveolin-1.

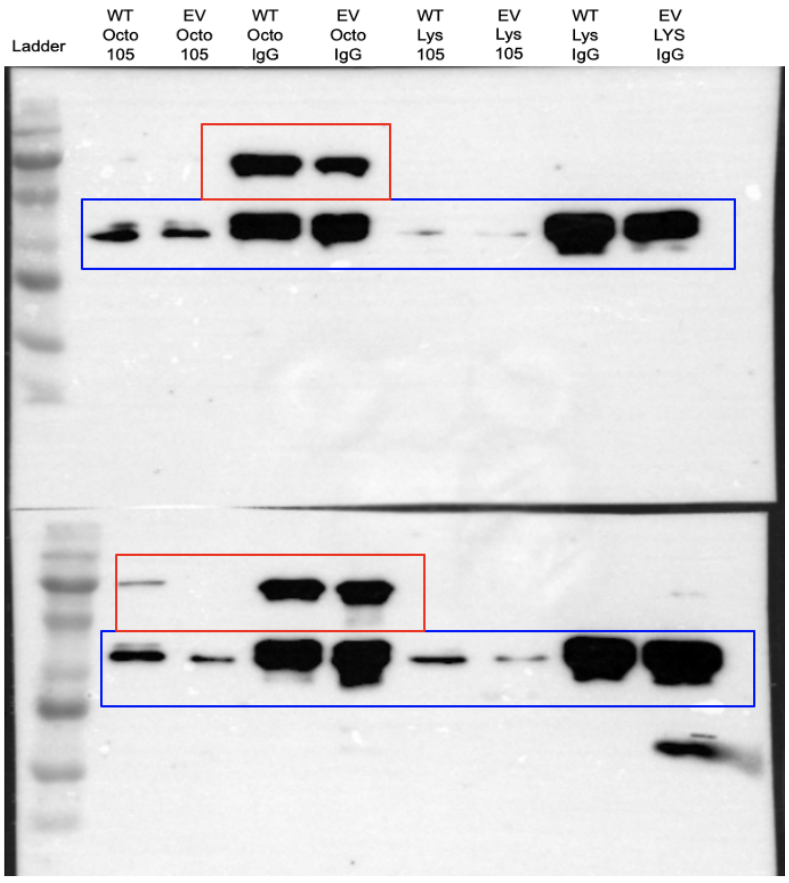

Figure 8. Western blot analysis of co-immunoprecipitation experiments where lanes are; 1. Molecular weight marker, 2. Cav+/mAb105/Octylglucoside buffer, 3. Cav-/mAb105/Octylglucoside buffer, 4. Cav+/IgG/Octylglucoside buffer, 5. Cav-/IgG/Octylglucoside buffer, 6. Cav+/mAb105/Lysis buffer, 7. CAV-/mAb105/Octylglucoside buffer, 8. Cav+/IgG/Lysis buffer, 9. Cav-/IgG/Lysis buffer. The top membrane was incubated with an anti-caveolin antibody. The bottom membrane was incubated with an anti-FSH antibody.

Before future studies are conducted, time should be devoted to finding the specific details of the successful co-immunoprecipitation procedure used by a previous research student. A former thesis student in the Cohen Lab was able to successfully show a physical association between FSHR and caveolin-1. After this procedure is found, a determination can be made as to whether the results of the respective experiments are an artifact of the protocol used. It is possible that changing the detergent used to lyse cells, or the stringency of the detergent may produce results consistent with previously collected data. Furthermore, a caveolin-1 specific antibody could be utilized to probe from caveolin instead of an antibody that binds to a caveolin protein with a myc-tag that was transfected in this experiment. Using a caveolin-1 specific antibody we can look for native as well as transfected caveolin rather than just non-native caveolin transfected with a myc-tag.

Overall, it was confirmed through western blot analysis of whole cell experiments that caveolin and hFSHR expressed in HEK293R cells cultured in the lab. FSHR was detected using anti-FSHR antibody and caveolin was detected using both an anti-caveolin antibody and . However, pulldown experiments did not produce visible bands consistent with hFSHR or caveolin. The bands that were detected were consistent with IgG antibodies. Despite prior data, a physical association between caveolin and hFSHR was not identified at this time.

Understanding the interaction between hFSHR and caveolin can provide a deeper understanding into hFSHR function and potential dysfunction. Having more knowledge about normal receptor function could allow for the development of biased agonists or antagonists to

allow us to fine tune receptor function for assisted reproduction technologies or for other infertility treatments.

Families struggling to conceive are forced to face astronomical expenses or the reality of a childless life. The associated emotional stress diminishes the quality of life for many (15). Those patients whose infertility may be caused by FSHR related mechanisms cannot yet be identified due to an insufficient understanding of signaling pathways.

Another perspective represents the millions of Americans who do not want to have children. The recent increase in intrauterine device (IUD) popularity demonstrates the growing need for birth control methods with minimal side effects than current hormonal methods (16). A deeper understanding of the FSH signaling pathways will allow for innovative family planning solutions that empower people to better choose when they begin or grow their families.

Appendices

Appendix I

After the cells were grown to confluence, cells were split onto 60 mm dishes. 500 microliters of serum free medium, 6.75 microliters of caveolin (1778 ng/uL), and 20 microliters of transit 293 were added to a microfuge tube and pipetted up and down gently. The contexts were allowed to incubate for 15 minutes. 250 microliters were added to each of two 60 mm dishes. Empty vector caveolin was transfected into the cells as a control.

Appendix II

Recipe for CHAPS:

Cell suspensions were diluted 4-fold in "CHAPS buffer," containing 50 mM Tris-HCl (pH 7.4), 20 mM CHAPS, 125 mM NaCl, 2 mM dithiothreitol, 0.1 mM EGTA, 4 μM tetrahydrobiopterin, 1 mM L-arginine and protease inhibitors as above

Appendix III

Recipe for Octylglucoside:

Combined 10 mM Tris-Cl, pH 8, 150 mM NaCl, 60 mM octyl glucoside, and 1 protease inhibitor pellet per 10ml.

Appendix IV

Recipe for 100 mL lysis buffer:

Combine, 1.0 mL Igepal CA-640, 0.4 g Sodium Deoxycholate, 20 mL 50mM Tris HCl, pH 7.4, 1 mL 500mM EDTA, 0.82 g Sodium Chloride or, 2.8 mL 5M Sodium Chloride, and add ddi water to final volume. Immediately before use aliquot the necessary amount and add protease and phosphatase inhibitors

Appendix V

After transferring the gel to a membrane using standard western blot techniques, the membrane was washed in 1x TBST three times in five minute intervals. Then, it was incubated with 20 mLs of 5% BSA overnight. The membrane was then blocked with unlabeled streptavidin in 5% BSA (100 microliters streptavidin/ 10ml 5% BSA) for one hour at room temperature. The membrane was then washed with 1x TBST 3 times, for 5 minutes. The membrane was then blocked with free biotin in 5% BSA (1 mg biotin/ 10 ml 5% BSA) for one hour at room temperature. The membrane was then washed with 1x TBST 3 times, for 5 minutes. The membrane was then probed with a biotinylated antibody in 5% BSA (10 microliters antibody/ 10ml 5% BSA) overnight at 4° C. The membrane was then washed with 1x TBST 3 times, for 5 minutes. The membrane was then probed with streptavidin-HRP in 5% BSA (10 microliters streptavidin-HRP/ 10ml 5% BSA) overnight at 4° C. The concentrations of all antibodies were 1mg/mL

Appendix VI

After transerfing the SDS-PAGE gel to a membrane, it was washed in 1x TBST three times in five minute intervals. Then, it was incubated with 20 mLs of 5% milk overnight. The membrane was then incubated with primary antibody in 5% BSA (2 microliters/ 10ml 5% BSA) overnight at 4° C. The membrane was then washed with 1x TBST 3 times, for 5 minutes. The membrane was then incubated with secondary in 5% BSA (2 mg secondary/ 10ml 5% BSA) overnight at 4° C. After, the membrane was washed a final time with 1x TBST 3 times, for 5 minutes. All membranes were developed using Lab Imager.

Appendix VII

A confluent 60mm dish of cells provides enough extract for at least 2 IPs. Do all steps on ice or at 4°C.

Rinse cells with 1X PBS, add 1.0 ml ice-cold octylglucoside buffer or lysis buffer/dish , incubate on ice for 10 min., harvest cells into microfuge tubes, dounce homogenize with 10 strokes (tight pestle), spin in microfuge at at 4°C, 13,000rpm for10 min, save supernatant.

Add 5ug Ab (105 or IgG2b), vortex gently, incubate at 4°C overnight (don't need to rock, etc.).

Add 100µL of protein A-agarose beads, incubate at 4°C for 2h with end-over-end rotation.

Underlay extract with 0.5ml cushion of 0.5x octylglucoside/30% sucrose or 0.5 x lysis

buffer/30% sucrose, microfuge for 20 seconds, remove supernatant

wash beads twice more with 0.5ml 0.5x octylglucoside buffer or lysis buffer.

Resuspend beads in 60µL 2x sample buffer, heat for 5 minutes at 75oC, centrifuge for 1 min at max speed, transfer supernatant to a new tube and store at -20°C.

References

1. Infertility FAQs [Internet].; 2019 [updated January 16,; cited 11-2-20]. Available from: https://www.cdc.gov/reproductivehealth/infertility/.
2. Infertility [Internet].; 2019 [updated July 25,; cited 11-2-20]. Available from: https://www.mayoclinic.org/diseases-conditions/infertility/diagnosis-treatment/drc-20354322.
3. Katz P, Showstack J, Smith J, Nachtigall R, Millstein S, Wing H, et al. Costs of infertility treatment: Results from an 18-month prospective cohort study. Fertility and Sterility Home. 2010 Dec 4;95(3).
4. Lu N, Matzuk MM, Wang Y, Kumar TR. Follicle stimulating hormone is required for ovarian follicle maturation but not male fertility. Nat Genet. 1997 Feb;15(2):201-4.
5. Holt R, Hanley N. Essential Endocrinology and Diabetes. 6th ed. Wiley Blackwell; 2012.
6. Huhtaniemi I. The Parkes lecture. Mutations of gonadotrophin and gonadotrophin receptor genes: what do they teach us about reproductive physiology? J Reprod Fertil. 2000 Jul;119(2):173-86.
7. Patel HH, Murray F, Insel PA. G-protein-coupled receptor-signaling components in membrane raft and caveolae microdomains. Handb Exp Pharmacol. 2008;(186)(186):167-84.
8. Hunzicker-Dunn M, Maizels ET. FSH signaling pathways in immature granulosa cells that regulate target gene expression: branching out from protein kinase A. Cell Signal. 2006 September;18(9):1351-9.
9. Byrne DP, Dart C, Rigden DJ. Evaluating caveolin interactions: do proteins interact with the caveolin scaffolding domain through a widespread aromatic residue-rich motif? PLoS One. 2012;7(9):e44879.
10. Wells M, Cohen B. Follicle Stimulating Hormone Receptor Signaling is Regulated by Lipid Raft Residency. The FASEB Journal. 2018 01 April;32.
11. Brown DA, London E. FUNCTIONS OF LIPID RAFTS IN BIOLOGICAL MEMBRANES. Annu Rev Cell Dev Biol. 1998 Nov;14(1):111-36.
12. Dart C. Lipid microdomains and the regulation of ion channel function. J Physiol. 2010 Sep 1;588:3169-78.
13. Lu TL, Kuo FT, Lu TJ, Hsu CY, Fu HW. Negative regulation of protease-activated receptor 1-induced Src kinase activity by the association of phosphocaveolin-1 with Csk. Cell Signal.

2006 November;18(11):1977-87.
14. Dominic PB, Dart C, Daniel JR. Evaluating Caveolin Interactions: Do Proteins Interact with the Caveolin Scaffolding Domain through a Widespread Aromatic Residue-Rich Motif? PLoS One. 2012 Sep 1,;7(9):e44879.
15. van Balen F, Bos HMW. The social and cultural consequences of being childless in poor-resource areas. Facts Views Vis Obgyn. 2009;1(2):106-21.
16. Yoost J. Understanding benefits and addressing misperceptions and barriers to intrauterine device access among populations in the United States. Patient Preference and Adherence. 2014 Jul 3,;8:947-57.